



Emergency repair of an RC bridge column with fractured bars using externally bonded prefabricated thin CFRP laminates and CFRP strips



Yang Yang^a, Lesley Sneed^{a,*}, M. Saiid Saiidi^b, Abdeldjelil Belarbi^c, Mo Ehsani^d, Ruili He^a

^a Department of Civil, Architectural and Environmental Engineering, Missouri University of Science and Technology, Rolla, MO, USA

^b Department of Civil and Environmental Engineering, University of Nevada, Reno, NV, USA

^c Department of Civil and Environmental Engineering, University of Houston, Houston, TX, USA

^d QuakeWrap, Inc., Tucson, AZ, USA

ARTICLE INFO

Article history:

Available online 21 July 2015

Keywords:

Bridge column
Carbon fiber reinforced polymer (CFRP)
Emergency repair
Fractured bars
Prefabricated laminates
Reinforced concrete (RC)

ABSTRACT

An emergency repair technique for a reinforced concrete (RC) bridge column that had buckled and fractured longitudinal bars was developed and assessed through an experimental study. The repair technique involved removing loose concrete, casting grout, cutting a trench around the base of the column in the footing, embedding carbon fiber reinforced polymer (CFRP) strips for flexural reinforcement, building a jacket from a prefabricated thin CFRP laminate, lowering the jacket into the trench bonding the CFRP composites to the column and the footing with pressurized epoxy, and restoring the strength of footing with externally bonded CFRP sheets. The repaired column was tested to failure under constant axial load and cyclic lateral load resulting in combined flexure, shear, and torsional moment loading. Test results showed that the repair method was successful in restoring the seismic performance of the column in terms of lateral strength and deformation capacity.

© 2015 Elsevier Ltd. All rights reserved.

1. Introduction

Reinforced concrete (RC) bridge columns designed according to current seismic design criteria are the major energy dissipating elements during earthquakes and may experience damage such as concrete spalling, concrete crushing, bar buckling, and/or bar fracture, which is usually localized at plastic hinge regions near column-footing or column-cap beam joints [1]. The other parts of the bridge such as cap beams, girders, and abutments are designed as capacity protected, i.e., these elements are designed to remain elastic during an earthquake without any damage. Therefore, the repair of damaged bridges to restore the traffic after a major earthquake usually involves repair of the columns. Prior to the 21st century, bar fracture was considered as unreparable, and thus little research had been conducted on the repair of RC columns with fractured bars. However, during the past decade, repair techniques for RC bridge columns with fractured bars have been developed and shown to be successful in restoring the column performance [2–11], although most techniques require a considerable amount of time and labor [12]. Among the methods described in the

literature, the use of externally bonded fiber reinforced polymer (FRP) composites has shown promise as an emergency repair method due to ease of construction and rapid achievement of material strength [4,5,7–9]. A wet-layup procedure has been used to apply the FRP, which involves concrete surface preparation, dry fiber saturation, wrapping of saturated fibers, and curing. In some cases where more than a few layers of FRP are required, the wet-layup procedure may take more than one day to complete [10] and extend the time required to complete the repair, which makes it less attractive in an emergency repair in which time to complete the repair is of critical importance. The wet-layup process also requires the replacement of any spalled concrete to create a smooth surface before the FRP is applied, which leads to further delay in the repair process. The major difference between an emergency repair and a permanent repair is that an emergency repair is designed to prevent further damage and accommodate essential traffic for disaster mitigation, whereas a permanent repair aims to restore the strength and deformation capacity of the damaged member to its original state. Accordingly, a lower limit state (or service level) may be expected for the case of an emergency repair than for a permanent repair.

Prefabricated FRP strips have traditionally been used to increase the flexural capacity of RC beams by externally bonding them to the tension side of the member [13]; they could also be used to

* Corresponding author. Tel.: +1 573 341 4553.

E-mail addresses: yuyt7@mst.edu (Y. Yang), sneedlh@mst.edu (L. Sneed), saiidi@unr.edu (M.S. Saiidi), abelarbi@central.uh.edu (A. Belarbi), mo@quakewrap.com (M. Ehsani), rhk82@mst.edu (R. He).

compensate for the flexural strength loss of columns with fractured longitudinal bars provided they can be adequately developed. However, little research has been reported on the application of prefabricated FRP strips in repair of damaged RC bridge columns. It should be noted that the rigidity of these strips, which are typically on the order of 0.05 in. (1.25 mm) thick, makes them suitable only for applications to relatively flat surfaces; i.e., the strips cannot be bent around a circular column.

Prefabricated FRP tubes or shells have been used in concrete-filled FRP tubes (CFFTs) with precast bridge columns in accelerated bridge construction (ABC). The prefabricated FRP tubes or shells are manufactured in a plant in a fixed shape and size and serve as stay-in-place (SIP) formwork for the concrete contained within, as well as longitudinal and transverse reinforcement in some cases [14–20]. Prefabricated FRP shells could also be wrapped around the surface of RC columns using a dry-layup procedure to repair damaged columns; however, this method has only been investigated for columns without fractured bars [21]. It is also noted that the FRP shells or jackets mentioned above are manufactured to a specific shape and size. As a result, they do not lend themselves to emergency repair applications where the size and shape of the column requiring repair is not known prior to the seismic event.

This paper proposes an emergency repair method for RC bridge columns with fractured longitudinal bars by using a combination of (1) externally bonded carbon-FRP (CFRP) strips and (2) a CFRP jacket in the column plastic hinge region that are inserted in a trench in the column footing. The jacket in this study uses a newly-developed form of FRP laminate [22] that has been used to repair deteriorated concrete piles [23]. Using a special process, one or more layers of carbon or glass fiber fabric are saturated in the plant and cured under pressure to produce thin flexible laminates that are supplied in rolls up to 5 ft (1.5 m) wide \times 300 ft (91 m) long. The thickness of the laminates is 0.02 in. (0.5 mm). In the field, the laminate can be cut to the desired length, coated with an epoxy paste, and then wrapped multiple times around a column of virtually any shape or size to create a multi-ply jacket or shell around the column. This unique construction leads to a jacket that has no weak seams along the height and that offers the same strength 360 degrees around the column. At this stage, the jacket is not bonded to the column and is free to move up or down along the column. This feature makes it easy for the jacket to be pushed into the footing provided that a narrow trench (e.g. 1 in. [25 mm] wide) is cut in the footing around the column.

To assess the effectiveness of the developed repair procedure, a 1/2-scale RC bridge column with fractured longitudinal bars was repaired with the proposed method and tested under constant axial loading and reversed cyclic lateral loading resulting in combined flexural, shear, and torsional effects. The overall goals of this paper are to demonstrate proof of concept and establish the details on the repair procedure and design philosophy. The performance of the repaired column is evaluated in terms of strength and deformation capacity, stiffness, energy dissipation, and measured strains.

2. Specimen description and damage

In a previous study, a 1/2-scale RC bridge column specimen was tested to failure under constant axial load and cyclic lateral loading [24]. In this paper, the original column is referred to as Calt-3. The column geometry and reinforcement details are shown in Fig. 1. The column had an oval-shaped cross section of 24 in. \times 36 in. (610 mm \times 915 mm), and the clear concrete cover to the spiral reinforcement was 1 in. (25 mm). The total height of the specimen was 166 in. (4.2 m) with an effective height of 132 in. (3.35 m) measured from the top of footing to the centerline of applied load,

with a resulting aspect ratio of 4.5. Longitudinal reinforcement was provided by 20 No. 8 bars (25.4 mm dia.) with a reinforcement ratio of 2.13%. Transverse reinforcement was provided by No. 4 (12.7 mm dia.) interlocking spirals with a pitch of 2.75 in. (70 mm) resulting in a transverse reinforcement volumetric ratio of 1.32%. Reinforcing bars were ASTM A706 [25]. The measured yield and ultimate strength of the longitudinal reinforcing bars was 76.7 ksi (529 MPa) and 104.1 ksi (717 MPa), respectively. The measured yield and ultimate strength of the spirals was 65.8 ksi (454 MPa) and 98.0 (676 MPa), respectively. The measured compressive strength of concrete was 5860 psi (40.4 MPa) on the test day. Concrete compressive strength was measured in accordance with ASTM C39 [26] using 6 in. \times 12 in. (15 mm \times 30 mm) cylinders.

The column was subjected to a constant axial load of 220 kips (979 kN), equivalent to 7% of the axial capacity of the column, and reversed cyclic lateral load resulting in combined bending moment, shear, and torsional moment. Bending was applied about an axis with an angle of 35 degrees to the weak axis (see Fig. 2). The torsional moment-to-bending moment (T/M) ratio was 0.2, which was designated in the previous study [24] with the objective to study the influence of the T/M ratio on the behavior of RC columns. The loading protocol for Calt-3 is shown in Fig. 3.

After the original test, the damage to the column was inspected visually and determined by analysis of measured data. As shown in Fig. 4, the concrete damage extended from the column base to a height of 39 in. (990 mm) above the top of footing. Four of the longitudinal bars buckled, and six of the longitudinal bars fractured. Buckled and fractured bars were located around the perimeter of the column on the extreme tension and compression sides. Measured strain data indicated that all of the longitudinal bars yielded. Yielding of the longitudinal bars was indicated by strain gages located in the region 4.0 in. (100 mm) to 61.75 in. (1570 mm) above the top of footing. Yielding may also have occurred within the footing but could not be verified since no strain gages were installed on the portion of the longitudinal bars inside the footing. Strain gages were also installed on the spirals, however most gages within the plastic hinge region stopped functioning prior to termination of testing. The strain values collected from those gages before they malfunctioned and from other sound strain gages did not exceed the yield strain of the spirals. However, yielding of spirals may have occurred near the base of the column for the reason that crushing of core concrete was observed and is usually considered to be a result of loss of confinement, which suggests that the spirals yielded.

3. Repair program

The objective of repairing Calt-3 was to restore the flexural, shear, and torsional strength of the column; thus the method was considered an emergency repair rather than a permanent repair that aims to restore the deformation capacity as well. The repaired column is referred to in this paper as R-Calt-3.

3.1. Repair materials

Repair grout with a similar compressive strength as the existing concrete was used to repair the plastic hinge region of the column. The measured compressive strength of grout was 6010 psi (41.4 MPa) on the test day. The compressive strength of grout was determined by 2 in. \times 2 in. \times 2 in. (50 mm \times 50 mm \times 50 mm) cubes tested according to ASTM C109 [27]. Three types of CFRP composites were used. CFRP strips bonded to the surface of the column were prefabricated with unidirectional carbon fibers. The material properties of the CFRP strips are listed in Table 1.

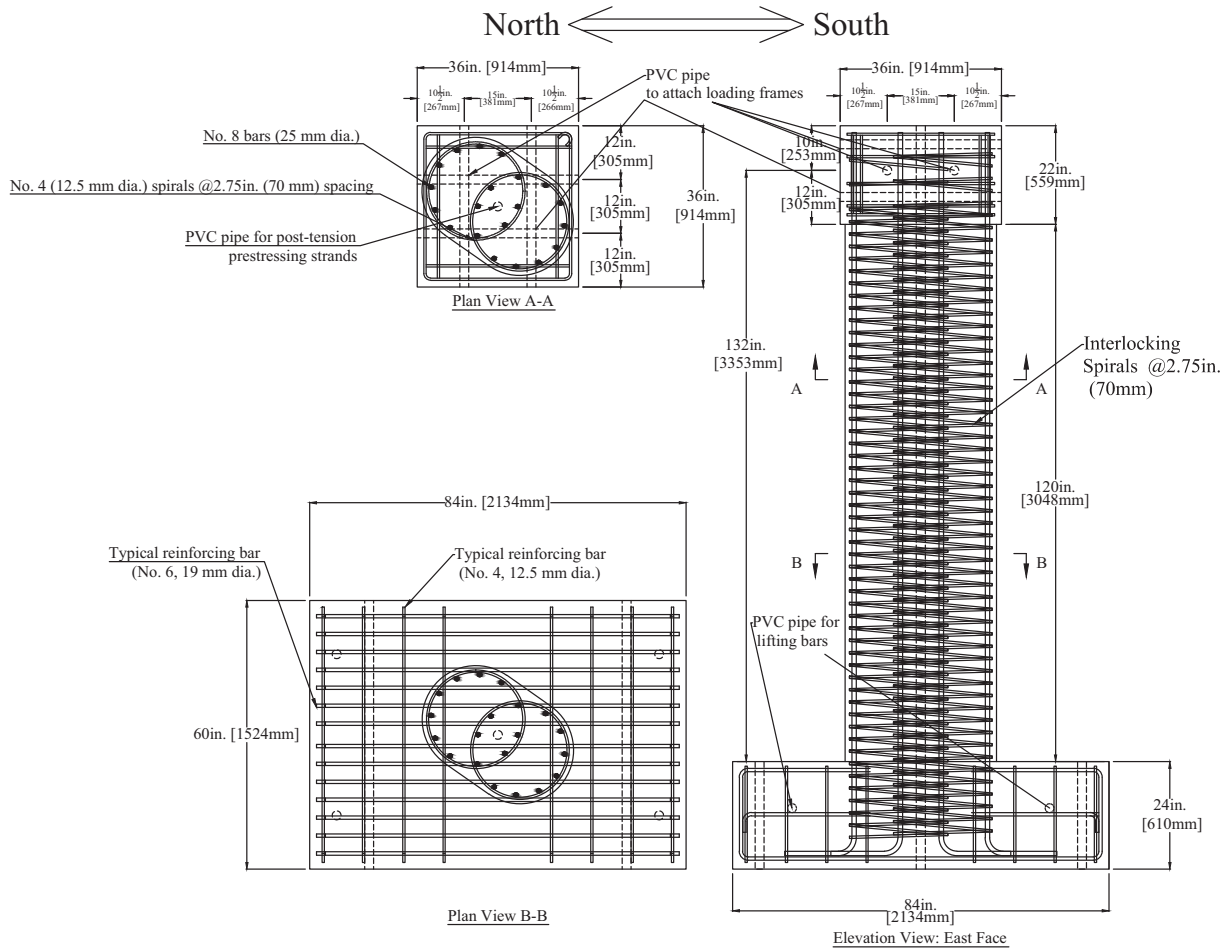


Fig. 1. Geometry and reinforcement details of Calt-3.

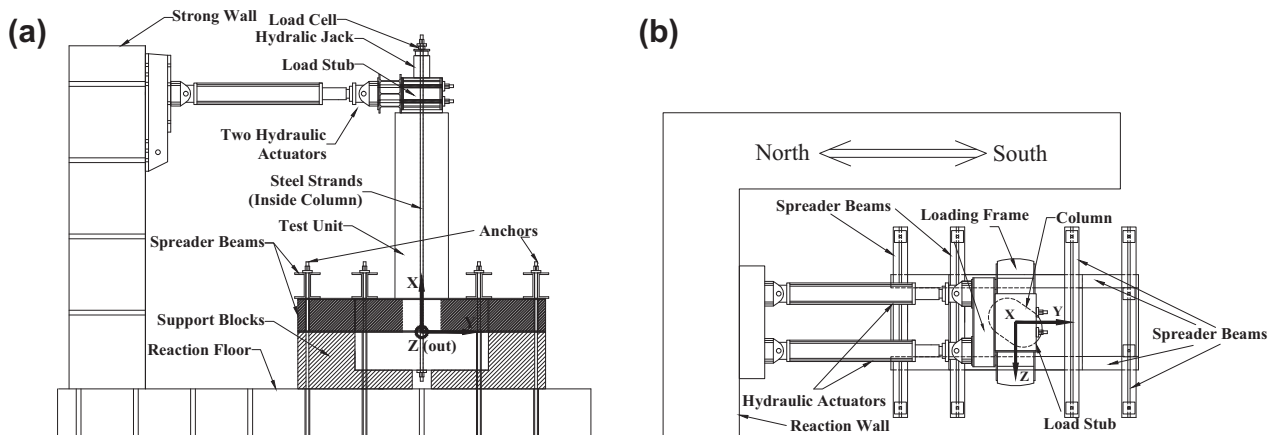


Fig. 2. Test setup. (a) Elevation view. (b) Plan view.

Unidirectional CFRP fabric with a density of 18.5 oz/sq yd (627 g/sq m) was used to repair the footing, and the material properties are listed in Table 2. The properties of the prefabricated CFRP laminates used to construct the jacket are listed in Table 3. An epoxy paste was used for the inter-layer bond of the CFRP jacket. Low-viscosity epoxy resin was used to bond the CFRP jacket to the repaired concrete surface and the footing. The properties of the epoxy resin are listed Table 4. The same epoxy was also used

with aggregate material to fill the trench in the footing outside the jacket (discussed in Section 3.3). 4 in. (100 mm) × 8 in. (200 mm) cylinders were cast from the epoxy-aggregate material. Splitting tensile tests and compression tests were conducted to determine the mechanical properties of this material according to ASTM C496 [28] and ASTM C39 [26]. The measured splitting tensile strength was 700 psi (4.8 MPa), and the measured compressive strength was 6930 psi (47.8 MPa).

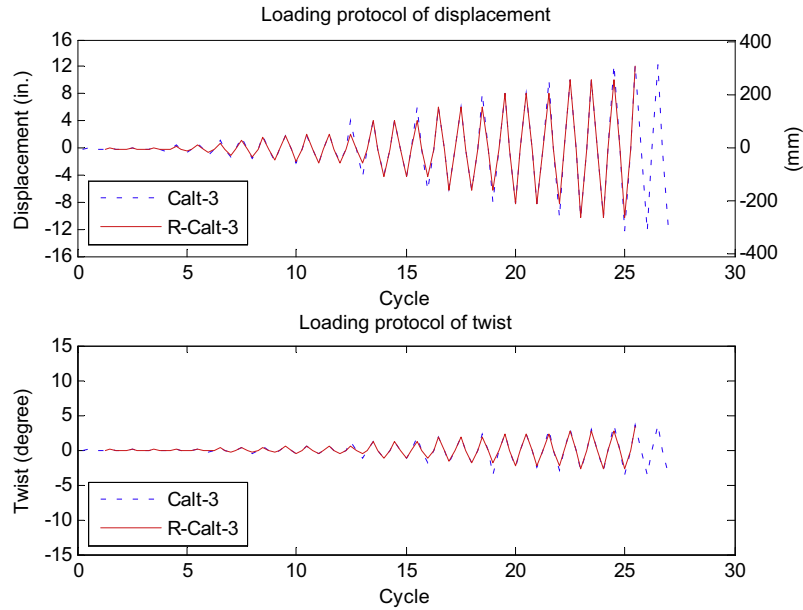


Fig. 3. Loading protocol of Calt-3 and R-Calt-3.

3.2. Repair design

3.2.1. Column repair – shear and torsion

Within the plastic hinge region, the thickness of the CFRP jacket (i.e., number of layers) in the transverse direction of the column was designed to contribute 50% of the shear and torsion resistance provided by the original transverse spiral reinforcement based on a study by Vosooghi and Saiidi, who found that yielded spirals in a plastic hinge region can partially contribute to the shear strength of damaged RC columns [29]. The contribution of the CFRP jacket to the shear resistance (V_j) was calculated using Eq. (1) [29]:

$$V_j = \frac{\pi}{2} (t_j E_j \varepsilon_j D) \quad (1)$$

where t_j , E_j , ε_j are the thickness, elastic modulus, and effective strain (taken as 0.004 in shear design) of the CFRP, respectively; and D is the dimension of the column in the bending direction.

The contribution of the CFRP jacket to the torsion resistance (T_{frp}) was calculated based on the method by Zureick et al. [30] in Eq. (2):

$$T_{frp} = N_e \alpha x_1 y_1 \quad (2)$$

where N_e is the effective tensile force per unit length in the CFRP defined in Eq. (3):

$$N_e = t_j E_j \varepsilon_j + \frac{1}{2} (N_w - t_j E_j \varepsilon_j) \quad (3)$$

and α is defined in Eq. (4):

$$\alpha = 0.66 + 0.33 \left(\frac{y_1}{x_1} \right) \leq 1.5 \quad (4)$$

where t_j , E_j , ε_j are the thickness, elastic modulus, and effective strain (taken as 0.004 in torsion design) of the CFRP; $N_w = 0.5N_{ult} \geq t_j E_j \varepsilon_j$; N_{ult} is the ultimate tensile force per unit length provided by the manufacturer; and x_1 , y_1 are the lesser and larger limits of the dimension of the cross-section, respectively. Based on this design procedure, five layers of CFRP were required in the transverse column direction within the plastic hinge region for shear and torsion resistance.

3.2.2. Column repair – flexure and confinement

CFRP strips were designed to compensate for the loss of flexural strength due to the fractured bars. The number of CFRP strips on each side of the column was designed to provide the equivalent breaking tensile force corresponding to the measured fracture strength of the fractured longitudinal bars on the corresponding side. Using this procedure, four 4 in. (100 mm) wide CFRP strips were required on each side of the column. The manufacturer of the CFRP jacket recommended that at least two layers be provided for confinement based on previous experience and constructability considerations; thus, seven layers of CFRP in total were designed in the transverse direction taking into account the design for shear and torsion discussed in Section 3.2.1. The flexural design with the seven-layer bidirectional CFRP jacket and four CFRP strips on the tension side was verified using moment–curvature analysis in which the model proposed by Samaan et al. [31] was used to define the stress–strain relationship of the FRP-confined concrete.

3.2.3. Embedment length of CFRP jacket and strips

Recent studies have investigated moment transfer of concrete-filled FRP tubes embedded into concrete footings and the embedment length required to achieve the failure mode of FRP rupture. Zaghî et al. [32] provided full fixity of a column–footing connection by embedding a CFFT into a footing with a length of 1.5 times the diameter of the tube in addition to anchoring the column longitudinal bars with 90-degree hooks. It is worth noting that normal strength concrete was used in the footing. Sadeghian and Fam [33] proposed a simplified equation to calculate the required embedment length to transfer the full moment without the use of dowel bars shown in Eq. (5):

$$\frac{X}{D} = 5.55 \frac{\tau_{\max}}{f'_c} \left(\sqrt{1 + 0.31 \frac{f'_c}{\tau_{\max}^2} \frac{M}{D^3}} - 1 \right) \quad (5)$$

where X is the minimum required embedment length; D is the diameter of a circular jacket; τ_{\max} is the bond strength between the CFRP jacket and footing concrete; M is the bending moment transferred to the footing; and f'_c is the compressive strength of concrete. Sadeghian and Fam [33] proposed a critical embedment length corresponding to simultaneous bond failure within the

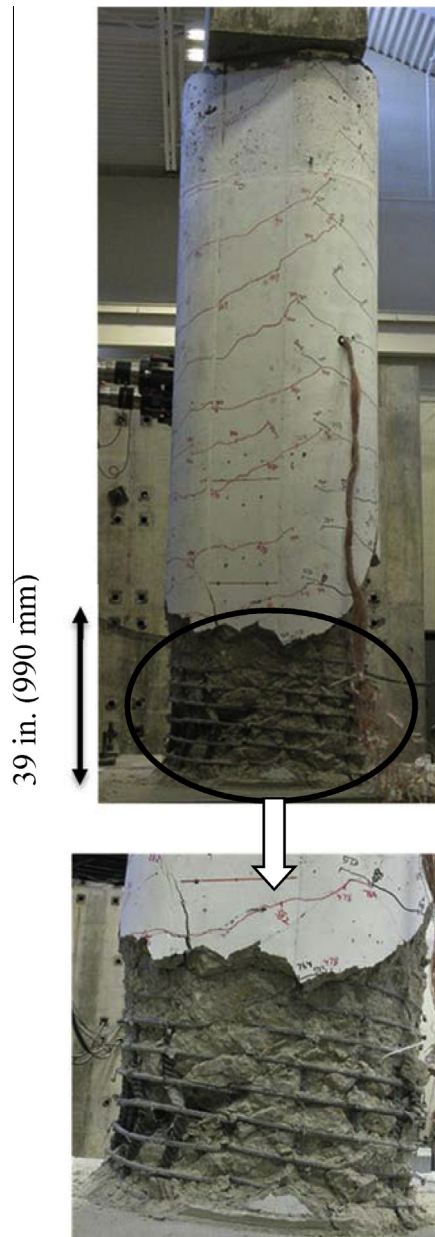


Fig. 4. Visible damage to concrete and reinforcement of Calt-3 after original test.

footing and material failure outside the footing of $0.7D$ and also mentioned that Eq. (5) is conservative when axial compressive load is present.

Assuming the full maximum bending moment of the repaired section was to be transferred to the footing by the CFRP jacket and strips, the required embedment length determined by Eq. (5) ranged from 16.6 in. (427 mm) to 28.6 in. (725 mm), depending on the direction of bending. Considering practical limitations, however, demolition of concrete into the footing with this depth would have further compromised the integrity of the footing, especially

Table 2
Properties of CFRP fabric (provided by manufacturer).

	US units	SI units
<i>Fiber properties</i>		
Tensile strength	550 ksi	3800 MPa
Tensile modulus	33,500 ksi	231,000 MPa
Ultimate elongation	1.64%	1.64%
<i>Fabric laminated with J300SR</i>		
Tensile strength	102.7 ksi	708 MPa
Tensile modulus	9950 ksi	68,600 MPa
Ultimate elongation	1.1%	1.1%
Ply thickness	0.0399 in.	1.01 mm

Table 3 Product used is: PileMedic PLC100.60
Properties of bidirectional prefabricated CFRP laminate (provided by manufacturer).

	US units	SI units
<i>Longitudinal (0°) direction</i>		
Tensile strength (ASTM D3039)	101 ksi	698 MPa
Modulus of elasticity (ASTM D3039)	7150 ksi	49,280 MPa
Ultimate elongation (ASTM D3039)	0.85%	0.85%
<i>Transverse (90°) direction</i>		
Tensile strength (ASTM D3039)	64.2 ksi	443 MPa
Modulus of elasticity (ASTM D3039)	2940 ksi	20,260 MPa
Ultimate elongation (ASTM D3039)	1.42%	1.42%
<i>Laminate properties</i>		
Ply thickness	0.026 in.	0.66 mm

Table 4 Product used is: QuakeBond 320LV
Properties of low viscosity resin epoxy (provided by manufacturer).

Tensile strength psi (MPa)	Compressive strength psi (GPa)	Elongation at break %	Adhesion to concrete psi (MPa)
7900 (54.5)	11,200 (77.2)	4.8	>800 (5.5); 100% failure in concrete

since additional layers of footing reinforcement might be damaged in the process. Thus, the CFRP embedment length was designed as 12 in. (305 mm) in this study, which was less than that estimated by the methods described above. Based on the repair design, the details of CFRP plates, CFRP jacket, and epoxy fill for the repaired column are illustrated in Fig. 5.

3.2.4. Footing repair

Several reinforcing bars in the footing needed to be cut to facilitate the embedment of the CFRP jacket and strips (shown in Fig. 5). Thus, CFRP fabric was externally bonded to the top surface of the footing to compensate for the loss of strength. Unidirectional CFRP fabric was cut into 12 in. (305 mm) wide straps to provide the required materials. The number of CFRP fabric layers was determined by the method proposed by Saini and Saiidi [34]. 10 layers of 12 in. (305 mm) wide CFRP straps were designed on four sides of the column, and the CFRP straps were extended to the side faces of the footing to secure the full development of the straps. The layout and orientation of the CFRP straps are shown in Fig. 6.

Table 1
Properties of unidirectional CFRP strips (provided by manufacturer).

Product used is: QuakeWrap GU50C

Tensile strength ksi (MPa)	Elongation at break %	Tensile modulus ksi (GPa)	Nominal laminate thickness in. (mm)	Width in. (mm)
400 (2758)	1.7	24,000 (165)	0.0472 (1.2)	4 (101.6)

PileMedic PLC 100.60

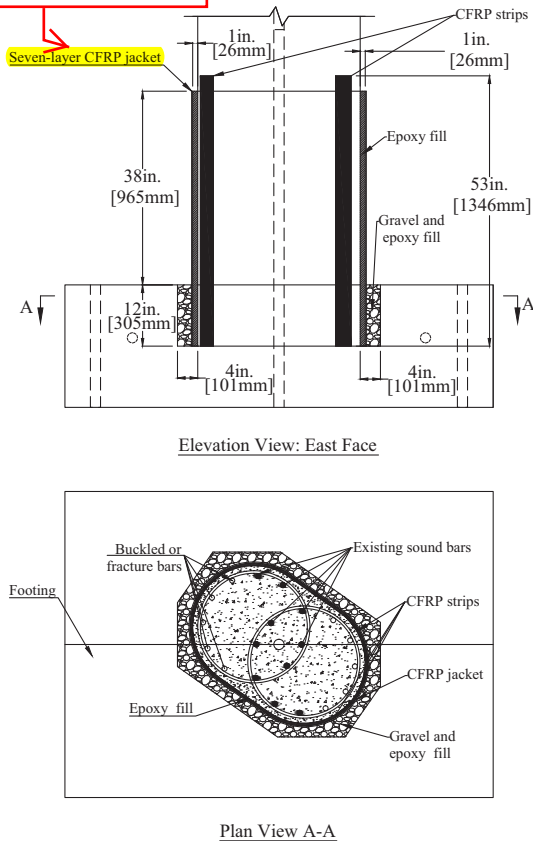


Fig. 5. Details of CFRP plates, CFRP jacket, and epoxy fill for R-Calt-3.

3.3. Repair procedure

The damaged column was relatively straight vertically and could support its own weight; thus, shoring and straightening was not conducted during the repair procedure. The repair procedure involved the following steps: (1) cutting a 4 in. (100 mm) wide and 12 in. (300 mm) deep trench around the base of the

column in the footing; (2) removing loose concrete from the column; (3) placing formwork and then a high-fluidity grout to restore the column cross-section; (4) installing CFRP strips on the column surface; (5) wrapping a 4 ft wide \times 60 ft long (1.2 m \times 18.3 m) epoxy-coated prefabricated laminate around the column to create a 7-ply jacket; (6) lowering the jacket into the trench until it touched the base of the trench; (7) filling the trench with an epoxy aggregate; (8) injecting a low-viscosity resin between the jacket and the column; and (9) installing CFRP fabric on the footing surface. Fig. 7 shows photos of the column during the repair procedure.

4. Test program

4.1. Test setup

The repaired column was subjected to the same cyclic lateral loading protocol and constant axial loading as applied to the original column. The test setup for R-Calt-3 is shown in Fig. 2 and is described in Section 2.

4.2. Instrumentation

Two load cells were integrated within the two actuators that measured force during testing. Load cells were also installed under the hydraulic jack on the top of column to record the variation of axial load. Two integrated direct current-linear voltage displacement transducers (DC-LVDTs) within the two actuators recorded the displacement during testing. Strain gages were installed on the surface of the CFRP jacket to measure both the longitudinal and transverse strains (refer to Fig. 8). Five levels of strain gages were also installed onto four of the CFRP strips before they were installed onto the column (refer to Fig. 9). Four strain gages were installed on the CFRP strips on each side of the footing to measure the surface strains of the CFRP (refer to Fig. 10).

4.3. Loading protocol

Before lateral loading was applied to the repaired column, axial loading was applied and kept constant during the entire test. The repaired column was subjected to reversed cyclic lateral loading

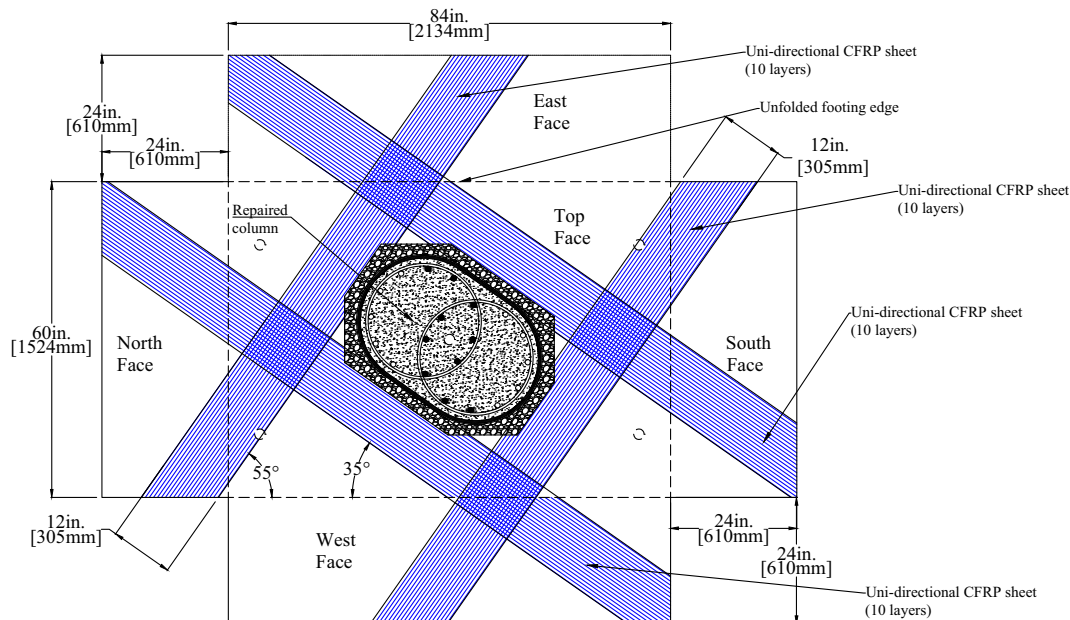


Fig. 6. CFRP strap layout on footing faces for R-Calt-3.

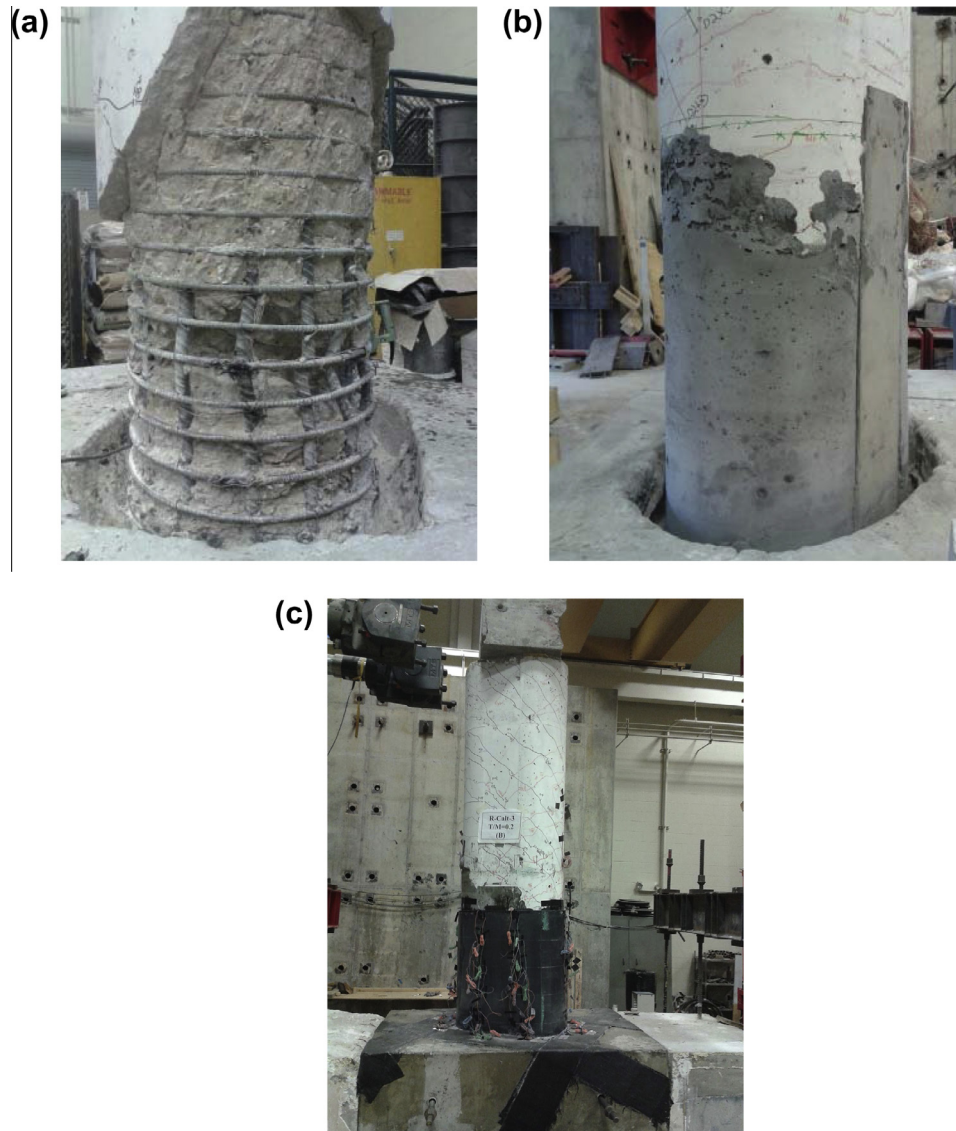


Fig. 7. Repair procedure for R-Calt-3. (a) Removal of loose concrete. (b) Grout placement. (c) R-Calt-3 prior to testing.

by controlling the displacement of the actuators. The first cycles included ten levels with one cycle per level, with the displacement corresponding to that of the force-control levels of the original column. After that, three cycles per each displacement level were applied to the repaired column with the same loading protocol as that of the original column. The loading protocol for both the repaired column and the original column is shown in Fig. 3.

5. Results and discussion

5.1. Observed damage

Testing of R-Calt-3 was terminated when the free end displacement of the column reached the maximum displacement applied to the original column. At a drift ratio of 2%, wrinkles in the CFRP jacket on the compression side of the column started to be noticeable. Inclined cracks in the concrete above the CFRP jacket from the original test were also widened at a drift ratio of 2%. At a drift ratio of 3%, vertical and inclined cracking were observed on both the east and west sides of the footing due to the shear and bending moment transferred to the footing. During loading to drift ratio of 3%, a loud

noise was heard that was later proved to be fracture of one of the existing longitudinal bars. The CFRP jacket started to rupture at a height of about 1 in. (25 mm) from the top of the footing on the compression side at a drift ratio of 3%, which explains the drop in lateral load at this level. Slip of the CFRP jacket from the footing was also noticed at this level. At higher levels (drift ratio > 3%), rupture of the CFRP jacket progressed and was observed on both sides of the column (see Fig. 11). Forensic inspection was conducted by removing the CFRP jacket after termination of test. Two bars that had buckled during the original test were observed as fractured. The CFRP strips were also found to have ruptured at a height of about 1 in. (25 mm) from the top of the footing during testing.

5.2. Base shear-lateral displacement and torsional moment-twist relationships

The base shear-lateral displacement hysteresis for R-Calt-3 and Calt-3 are compared in Fig. 12(a), where “push” was defined as positive and “pull” as negative. The hysteretic behavior of R-Calt-3 was asymmetric with higher maximum base shear in the push direction than in the pull direction. This may be due to

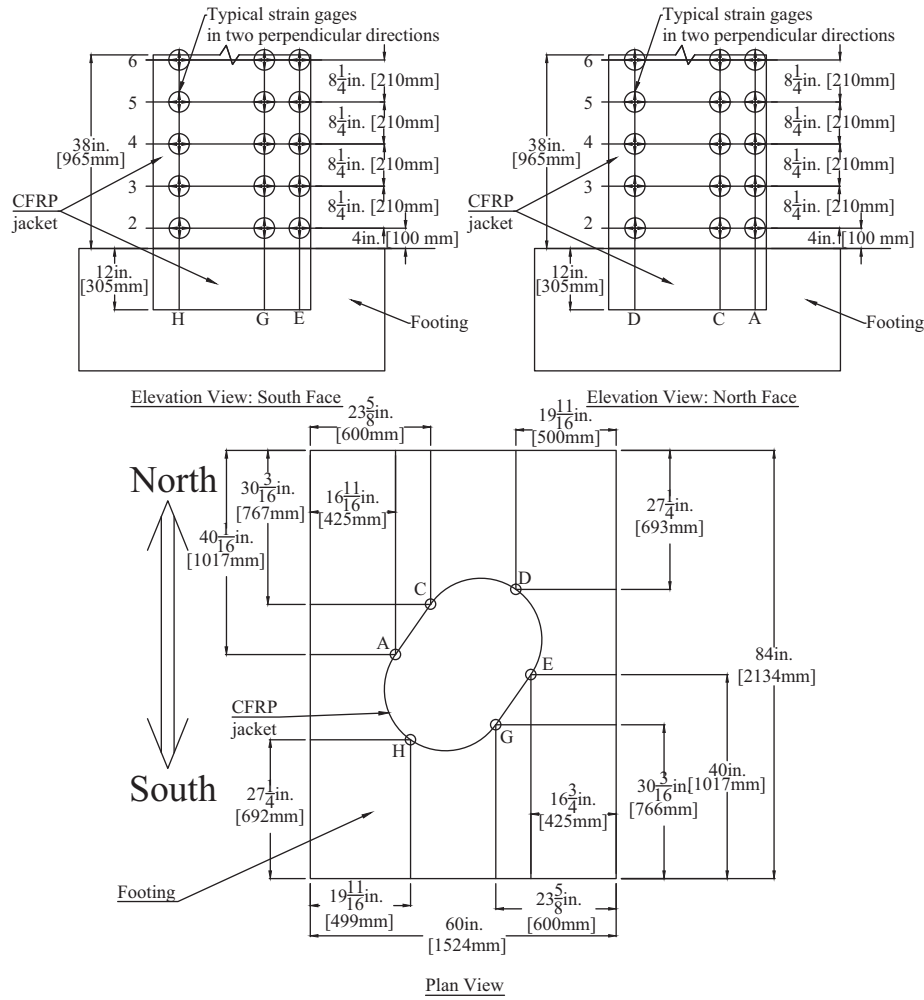


Fig. 8. Strain gage layout on CFRP jacket for R-Calt-3.

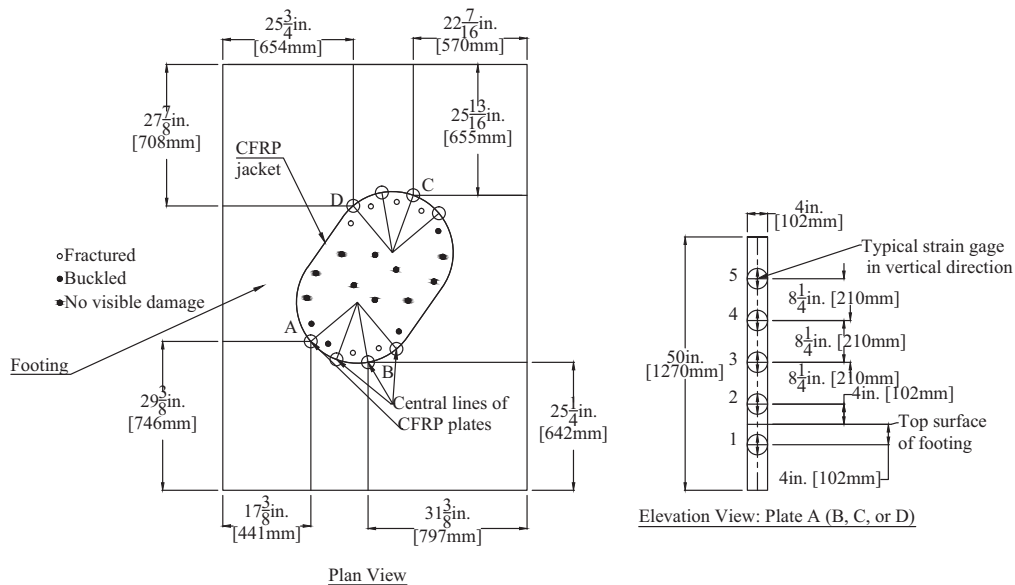


Fig. 9. Strain gage layout on CFRP strips for R-Calt-3.

the fact that the rupture of CFRP jacket of R-Calt-3 in the positive cycle reduced the load capacity in the subsequent negative cycle. It should be noted that the higher maximum lateral displacement

applied in the push direction was due to the fact that the actuators had a larger stroke capacity in the push direction than in the pull direction. The maximum positive base shear of R-Calt-3 was larger

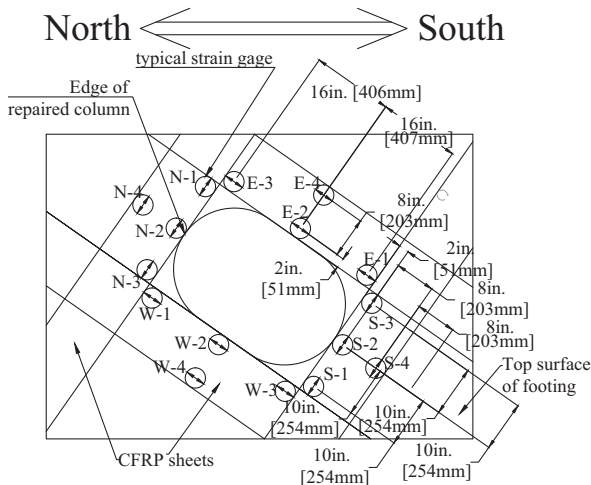


Fig. 10. Strain gage layout on CFRP straps on footing.



Fig. 11. CFRP rupture on column tension side at drift ratio of 3% (R-Calt-3).

than that of Calt-3. The lateral strength of R-Calt-3 started to degrade at 4 in. (100 mm) corresponding to a drift ratio 3% in both directions due to rupture of the CFRP jacket. This was similar to the response of Calt-3, which started to degrade at a displacement of 4 in. (100 mm) corresponding to a drift ratio 3% in both directions. However, the strength degradation rate of R-Calt-3 was much higher than that of Calt-3. This may be due to the brittle behavior of the longitudinal CFRP strips. The cyclic loops of R-Calt-3 had a similar shape as those of Calt-3 with similar unloading stiffness before strength degradation of both columns. The pinching effect was more noticeable in R-Calt-3 than in Calt-3.

Base shear and lateral displacement envelopes for R-Calt-3 and Calt-3 are compared in Fig. 13(a). The initial lateral stiffness of R-Calt-3 was lower than that of Calt-3 in both directions. This

may have been due to slippage of the CFRP jacket relative to the substrate since the adhesive layer was as thick as 1 in. (22 mm) in places and had a much lower stiffness than both the CFRP and concrete. Table 5 summarizes the maximum base shear in both directions. Idealized envelopes representing an elasto-plastic curve for Calt-3 and R-Calt-3 are also compared in Fig. 13(a). The bilinear envelopes were idealized by setting the initial slope to pass through the first yield point recorded during testing of Calt-3 and adjusting the plastic portion to equate the areas under the measured and idealized curves. Table 6 summarizes the critical values obtained from the idealized envelopes. In Table 6, the equivalent yield base shear (or torsional moment) is the average value of yield base shears (or torsional moments) in both directions. The equivalent lateral (or torsional) stiffness is the average value of the stiffness calculated in both directions. The equivalent lateral (or torsional) ductility ratio is the average value in the both directions. As shown in Table 6, the equivalent yielding lateral force, the equivalent elastic lateral stiffness, and the equivalent lateral ductility ratio of R-Calt-3 was approximately 92%, 95%, and 98% of that of Calt-3, respectively. This indicates that the repair method was successful in restoring the lateral behavior of the column.

Fig. 12(b) shows the hysteresis of torsional moment and twist, where clockwise torsion is defined as positive and counterclockwise torsion as negative. Degradation of the torsional strength of R-Calt-3 was observed at an angle of 2.5 degrees corresponding to a twist per unit length of 0.02 degrees/in. in the positive direction, while no degradation of the torsional strength of R-Calt-3 was observed in the negative direction. Torsional moment and twist envelopes of R-Calt-3 and Calt-3 are compared in Fig. 13(b). The initial torsional stiffness of R-Calt-3 was much lower than that of Calt-3. This may be due to relative movement (slip) between the CFRP jacket and the column due to the low modulus of the epoxy filled in between them. Elasto-plastically idealized torsional moment and twist curves are shown in Fig. 13(b), from which critical values were calculated and summarized in Table 6. The equivalent yield torque of R-Calt-3 was 97% of that of Calt-3, while the equivalent elastic torsional stiffness and torsional ductility ratio of R-Calt-3 was only 36% and 28% of that of Calt-3, respectively. This indicates that the repair method was successful in restoring the torsional strength; however, it did not restore the torsional stiffness and ductility.

5.3. Energy dissipation

The energy dissipation for both the repaired and original columns is shown in Fig. 14(a). The energy dissipation per cycle of R-Calt-3 was lower than that of the Calt-3. Also, the energy dissipation of R-Calt-3 at different drift ratios was lower than that of Calt-3. Cumulative energy dissipation is compared between the original and repaired columns in Fig. 14(b). The repaired column showed smaller cumulative energy dissipation at end of each load cycle than the original column. This is attributed to the brittleness of the CFRP reinforcement and the significant amount of plastic deformation that had already occurred in the internal steel reinforcement during the original test. The cumulative energy dissipation at different drift ratios of R-Calt-3 was also lower than that of Calt-3.

5.4. Measured strains

The maximum measured tensile strain in the longitudinal fibers of the CFRP jacket was at location "H" of the cross-section (defined in Fig. 8) at a height of 4 in. (100 mm) above the top of the footing. The maximum value was measured at a drift ratio of -2% and was close to 0.008, which is 56% of the rupture strain in that direction (0.0142 provided by the manufacturer, refer to Table 3). The

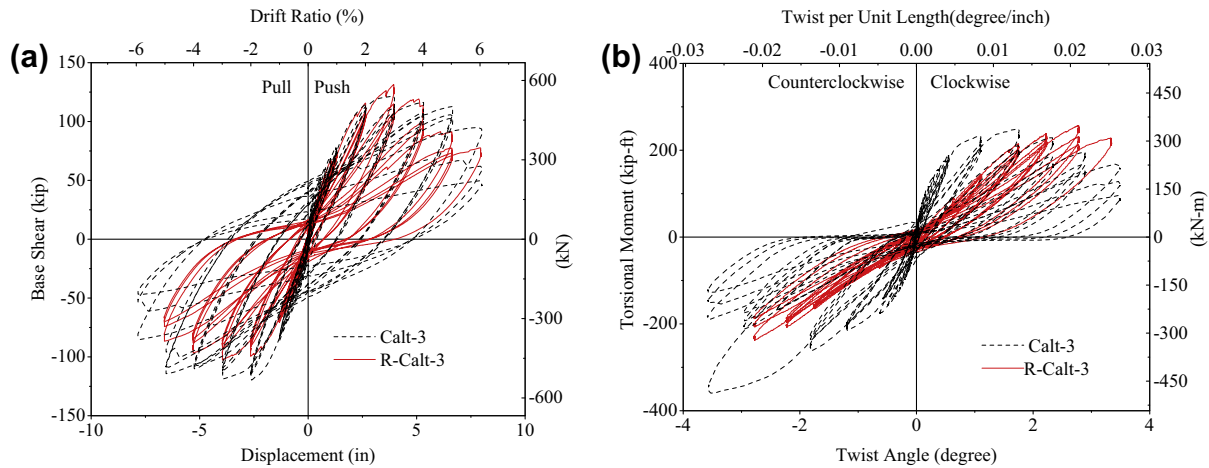


Fig. 12. Load–displacement hysteresis responses of Calt-3 and R-Calt-3. (a) Base shear vs. displacement. (b) Torsional moment vs. twist angle.

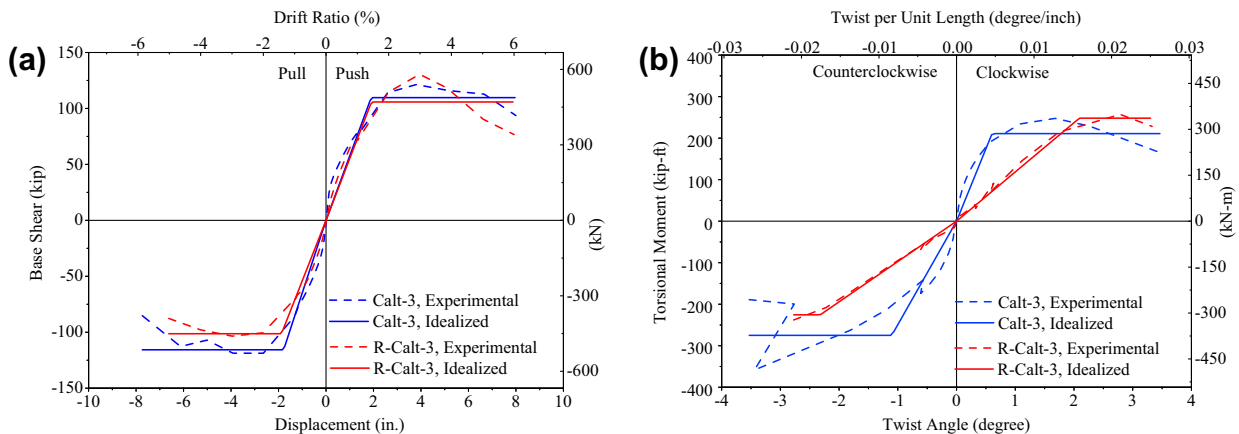


Fig. 13. Experimental and idealized load–deformation envelopes of Calt-3 and R-Calt-3. (a) Base shear vs. displacement. (b) Torsional moment vs. twist angle.

Table 5
Summary of measured forces of Calt-3 and R-Calt-3.

Column ID	Maximum positive base shear kip (kN)	Maximum negative base shear kip (kN)	Maximum positive torsional moment kip-ft (kN-m)	Maximum negative torsional moment kip-ft (kN-m)
Calt-3	121.4 (540.0)	118.7 (528.0)	247.6 (342.3)	358.4 (485.9)
R-Calt-3	130.5 (580.5)	103.5 (460.4)	257.1 (348.6)	238.0 (322.7)

Table 6
Critical values on idealized load–displacement curves.

Column ID	Equivalent average yielding base shear kip (kN)	Equivalent average yielding torsional moment kip-ft (kN-m)	Equivalent average lateral stiffness kip/in (kN/mm)	Equivalent average torsional stiffness kip-ft/rad (kN-m/rad)	Equivalent lateral ductility ratio	Equivalent torsional ductility ratio
Calt-3	112.7 (501.3)	243.0 (329.5)	56.0 (9.79)	16,979 (23,020)	4.1	5.8
R-Calt-3	103.6 (460.8)	236.8 (321.1)	53.4 (9.33)	6175 (8372)	4.0	1.6

maximum measured compressive strain in the longitudinal fibers of the CFRP jacket was 0.008 at a drift ratio of +5% at a location of “H” at a height of 12.25 in. (310 mm) from the top of the footing. The measured strain values indicate no rupture of CFRP in the region instrumented with strain gages, which was consistent with the observation during testing that rupture of CFRP occurred within a region no higher than 2 in. (50 mm) from the top of the footing.

Strains measured in the transverse fibers of the CFRP jacket were mainly tensile strains. The maximum tensile strain was measured at location “E” (defined in Fig. 8) at a drift ratio of +5% at a height of 4 in. (100 mm) above the top of the footing. The measured value was between 0.008 and 0.01, which was close to the rupture strain of the CFRP jacket in that direction (0.0085 provided by the manufacturer, Table 3).

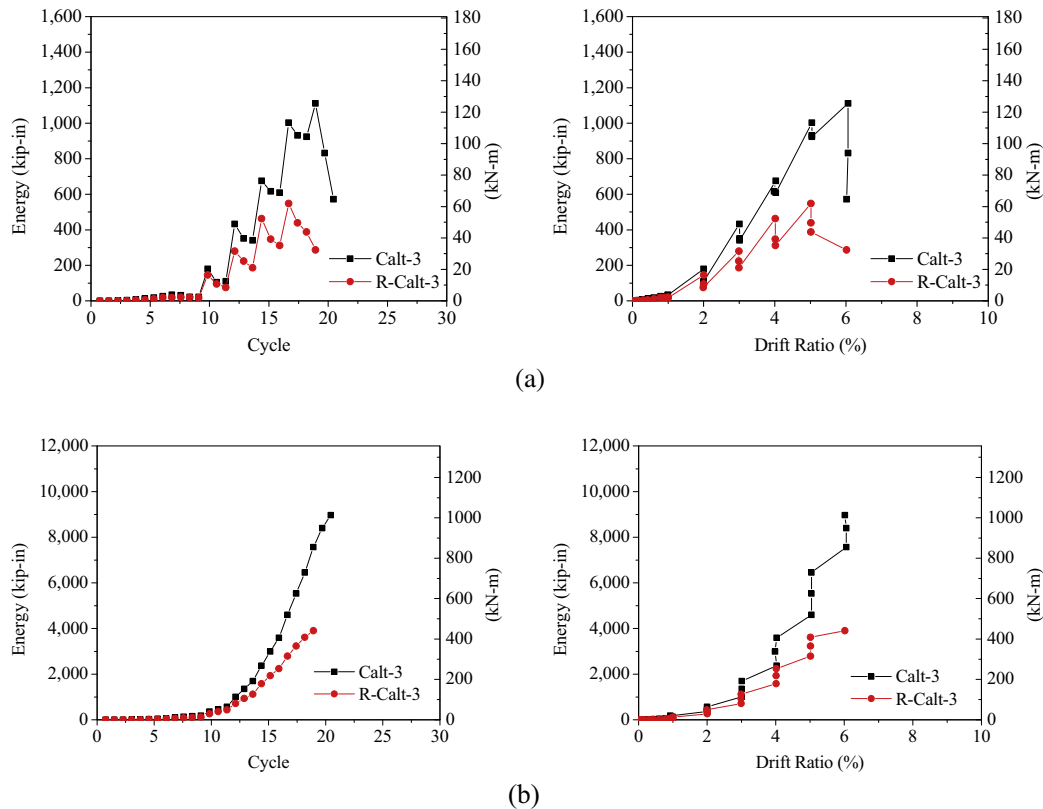


Fig. 14. Energy dissipation per cycle and cumulative energy dissipation of Calt-3 and R-Calt-3. (a) Energy dissipation per cycle. (b) Cumulative energy dissipation.

The maximum tensile strain in the CFRP strips was measured at location “B” (defined in Fig. 9) at a drift ratio of +3% at a height of 4 in. (100 mm) above the top of footing. The maximum measured strain was 0.006, which was 35% of the rupture strain provided by the manufacturer (refer to Table 1). The strain gages at this location malfunctioned at higher drift ratios, and no additional data could be recorded. However, it should be noted that the strains in the CFRP strips at the column-footing joint might be higher than that at the 4 in. (100 mm) high location because the plates ruptured at the base of the column as discussed in Section 5.1. The maximum measured compressive strain in the CFRP strips was 0.006 at a drift ratio of +3% at location “C”. Strain measurements from gages mounted 4 in. (100 mm) below top of footing indicated that the strain penetrated into the footing with a maximum tensile strain of 0.003 and maximum compressive strain of 0.005 measured at location “B”.

The maximum measured tensile strain in the CFRP straps bonded on the footing was between 0.0015 and 0.002, which was 38–50% of the design effective strain of 0.004.

6. Conclusions

This paper developed and assessed a method using externally bonded prefabricated CFRP laminates for emergency repair of damaged RC bridge columns with fractured bars through an experimental program. Based on the discussions and observations presented in this paper, the following conclusions are made:

1. The repair method was able to restore the lateral strength, stiffness, and ductility to the column, which suggests that it might also be applicable for the case of a permanent repair. However, the performance of this repair method depends on the bond provided by the epoxy that was filled in between the column

and the CFRP jacket as well as the column-footing joint integrity provided by the aggregate-filled epoxy within the trench. Therefore, long-term durability and bond performance of the epoxy and epoxy-aggregate should be investigated for the case of a permanent repair.

2. The repair method restored the torsional strength but resulted in a lower torsional stiffness and ductility compared to that of the original column.
3. Energy dissipation per cycle as well as cumulative energy dissipation of the repaired column were lower than that of the original column.
4. The design method for the transverse CFRP in this study was adequate and precluded damage to the transverse carbon fibers in the jacket.
5. The footing repair was successful and effective with no observed debonding of CFRP from the footing.
6. Since stiffness and energy dissipation of the repaired column were different from that of the original column, more work is needed to investigate the influence of the repair method on the response of the bridge structure.

Acknowledgement

The research reported herein was sponsored by the California Department of Transportation (Caltrans) Contract No. 65A0388 and the National University Transportation Center (NUTC) at the Missouri University of Science and Technology (Missouri S&T) Grant No. DTRT06-G-0014. The experimental research was performed by Missouri S&T. Major contributions to the project were made by Ashkan Vosooghi (post-doctoral researcher at University of Nevada, Reno), who contributed to the design of the repair, and Adam Morgan, Kristian Krc (graduate students at Missouri

S&T), and Wei Ren (visiting scholar at Missouri S&T), who contributed to the experimental work. Joshua Ahumada (QuakeWrap Inc.) contributed to the installation of the CFRP. Carbon fiber reinforced polymer composites were donated by QuakeWrap Inc. Shoring towers and pumping services were donated by Goedecke. Prospect Steel Company donated materials for the test setup.

References

- [1] Priestley MJN, Seible F, Calvi GM. Seismic design and retrofit of bridges. John Wiley & Sons; 1996.
- [2] Lehman DE, Gookin SE, Nacamuli AM, Moehle JP. Repair of earthquake-damaged bridge columns. *ACI Struct J* 2001;98(3):233–8.
- [3] Cheng C-T, Yang J-C, Yeh Y-K, Chen S-E. Seismic performance of repaired hollow-bridge piers. *Construct Build Mater* 2003;17(5):339–51.
- [4] Saiidi MS, Cheng Z. Effectiveness of composites in earthquake damage repair of reinforced concrete flared columns. *J Compos Construct* 2004;8(4):306–14.
- [5] Belarbi A, Silva PF, Bae S-W. Retrofit using CFRP composites of RC bridge columns under combined loads. In: Proc. 4th int. symp. on FRP composites in civil engineering (CICE). Switzerland: EMPA Duebendorf; 2008.
- [6] Shin M, Andrawes B. Emergency repair of severely damaged reinforced concrete columns using active confinement with shape memory alloys. *Smart Mater Struct* 2011;20(6):065018.
- [7] He R, Grelle S, Sneed LH, Belarbi A. Rapid repair of a severely damaged RC column having fractured bars using externally bonded CFRP. *Compos Struct* 2013;101:225–42.
- [8] He R, Sneed LH, Belarbi A. Rapid repair of severely damaged RC columns with different damage conditions – an experimental study. *Int J Concr Struct Mater* 2013;7(1):35–50.
- [9] Rutledge ST, Kowalsky MJ, Seracino R, Nau JM. Repair of reinforced concrete bridge columns containing buckled and fractured reinforcement by plastic hinge relocation. *J Bridge Eng* 2014;19(8).
- [10] Yang Y, Sneed L, Saiidi M, Belarbi A. Repair of earthquake-damaged bridge columns with interlocking spirals and fractured bars, Caltrans, final report CA 14-2179. Missouri University of Science and Technology, University of Nevada, University of Houston; July 2014.
- [11] Yang Y, Sneed LH, Morgan A, Saiidi MS, Belarbi A. Repair of RC bridge columns with interlocking spirals and fractured longitudinal bars – an experimental study. *Construct Build Mater* 2015;78(2015):405–20.
- [12] He R, Yang Y, Sneed LH. Seismic repair of reinforced concrete bridge columns: a review of research findings. *J Bridge Eng* 2015. [http://dx.doi.org/10.1061/\(ASCE\)BE.1943-5592.0000760](http://dx.doi.org/10.1061/(ASCE)BE.1943-5592.0000760).
- [13] ACI Committee 440. 440.2 R-08: Guide for the design and construction of externally bonded FRP systems for strengthening concrete structures. Farmington Hills, MI: American Concrete Institute; 2008.
- [14] Mirmiran A, Shahawy M, Samaan M. Strength and ductility of hybrid FRP-concrete beam-columns. *J Struct Eng* 1999;125(10):1085–93.
- [15] Shao Y, Mirmiran A. Experimental investigation of cyclic behavior of concrete-filled fiber reinforced polymer tubes. *J Compos Construct* 2005;9(3):263–73.
- [16] Zhu Z, Mirmiran A, Saiidi M. Seismic performance of reinforced concrete bridge substructure encased in fiber composite tubes. *Transp Res Rec J Transp Res Board* 2006;1976(1):197–206.
- [17] Fam A, Cole B, Mandal S. Composite tubes as an alternative to steel spirals for concrete members in bending and shear. *Construct Build Mater* 2007;21(2):347–55.
- [18] Ozbakkaloglu T, Saatcioglu M. Seismic performance of square high-strength concrete columns in FRP stay-in-place formwork. *J Struct Eng* 2007;133(1):44–56.
- [19] Sadeghian P, Lai Y, Fam A. Testing and modeling of a new moment connection of concrete-filled FRP tubes to footings under monotonic and cyclic loadings. *J Compos Construct* 2011;15(4):653–62.
- [20] Sadeghian P, Fam A. Closed-form model and parametric study on connection of concrete-filled FRP tubes to concrete footings by direct embedment. *J Eng Mech* 2011;137(5):346–54.
- [21] Saadatmanesh H, Ehsani MR, Jin L. Repair of earthquake-damaged RC columns with FRP wraps. *ACI Struct J* 1997;94:206–15.
- [22] Ehsani M. FRP super laminates. *Concr Int* 2010;32(03):49–53.
- [23] Ehsani M, Tipnis A. Miami building first to benefit from innovative pile jacket. *Concr Repair Bull* 2011;23(4):16–8.
- [24] Li Q, Belarbi A. Seismic behavior of RC columns with interlocking spirals under combined loadings including torsion. *Proc Eng* 2011;14:1281–91.
- [25] ASTM, A706/A706M-09b. Standard specification for low-alloy steel deformed and plain bars for concrete reinforcement. West Conshohocken, PA: ASTM International; 2009.
- [26] ASTM, C39/C39M-12a. Standard test method for compressive strength of cylindrical concrete specimens. West Conshohocken, PA: ASTM International; 2012.
- [27] ASTM, C109/C109M. Standard Test Method for Compressive Strength of Hydraulic Cement Mortars (Using 2-in. or [50-mm] Cube Specimens). West Conshohocken, PA: ASTM International; 2013.
- [28] ASTM, C496/C496M. Standard test method for splitting tensile strength of cylindrical concrete specimens. West Conshohocken, PA: ASTM International; 2011.
- [29] Vosoghi A, Saiidi MS. Design guidelines for rapid repair of earthquake-damaged circular RC bridge columns using CFRP. *J Bridge Eng* 2013;18(9):827–36.
- [30] Zureick AH, Ellingwood BR, Nowak AS, Mertz DR, Triantafillou TC. Recommended guide specification for the design of externally bonded FRP systems for repair and strengthening of concrete bridge elements, NCHRP report 655. Washington, DC: Transportation Research Board; 2010.
- [31] Samaan M, Mirmiran A, Shahawy M. Model of concrete confined by fiber composites. *J Struct Eng* 1998;124(9):1025–31.
- [32] Zaghi AE, Saiidi MS, Mirmiran A. Shake table response and analysis of a concrete-filled FRP tube bridge column. *Compos Struct* 2012;94(5):1564–74.
- [33] Sadeghian P, Fam A. Bond-slip analytical formulation toward optimal embedment of concrete-filled circular FRP tubes into concrete footings. *J Eng Mech* 2010;136(4):524–33.
- [34] Saini A, Saiidi MS. Post-earthquake damage repair of various reinforced concrete bridge components. In: Draft progress report to caltrans post-earthquake bridge damage mitigation. Reno, NV: Department of Civil and Environmental Engineering, University of Nevada, Reno; 2013.

The repair technique and materials described in this paper are proprietary and covered by U.S. Patents #8,650,831, #9,376,782 and other pending U.S. and international patent applications.